

## EVIDENCE FOR LARGE-SCALE SOLAR MAGNETIC RECONNECTION FROM RADIO AND X-RAY MEASUREMENTS

P. K. MANOHARAN,<sup>1,2</sup> L. VAN DRIEL-GESZTELYI,<sup>1,3</sup> M. PICK,<sup>1</sup> AND P. DÉMOULIN<sup>1</sup>

*Received 1996 February 26; accepted 1996 June 10*

### ABSTRACT

Utilizing *Yohkoh* Soft X-ray Telescope and Nançay radioheliograph data, we present, for the first time, observations of expanding twisted X-ray loops and a series of nonthermal radio bursts that follow the loop expansion in time and space up to  $\sim 12'$  distance. The loops were produced during a long-duration C4.7 flare close to disk center on 1994 October 25 at 1049 UT. The series of radio bursts were observed on the southern hemisphere above a weak positive-polarity region. The Kitt Peak magnetogram shows the existence of a weak negative-polarity region on the northern hemisphere at the same heliolongitude. Simultaneously with the nonthermal radio bursts, we observed the appearance of two remote X-ray brightenings and subsequent formation of two coronal holes above these weak (quiet) magnetic regions of opposite polarity, which strongly suggest the involvement of these remote regions in the event. During the 6 hr-long gradual phase of the flare, new X-ray loop connections developed among the active region and the remote quiet regions. A nonthermal radio continuum emission originating from the active region was also observed.

We propose that the series of radio bursts, two remote X-ray brightenings, and new coronal loop connections were all signatures of a large-scale reconnection process between the expanding twisted flare loops and overlying transequatorial loops connecting quiet-Sun regions. The reconnection was only partial; the external part of the overlying large-scale fields were pushed out in the solar wind by the expanding twisted loops, leading to the formation of the coronal holes. The interaction between the active region and the large-scale fields seemed to be active during the entire gradual phase of the flare. This scenario may also explain the measurement of high-energy electrons in the interplanetary medium from  $74^\circ$  south heliolatitude as observed by *Ulysses*.

**Subject headings:** interplanetary medium — Sun: corona — Sun: flares — Sun: magnetic fields — Sun: radio radiation — Sun: X-rays, gamma rays

### 1. INTRODUCTION

The solar corona is extremely complex. Besides active region loops, there are loops, even transequatorial ones, interconnecting different active regions, and we see loop connections of active regions to quiet-Sun sites several arc-minutes away (Strong et al. 1994; Strong 1994). When a structure becomes unstable and starts expanding, it will very probably meet and interact with other magnetic loops. Such events may lead to a reorganization of the coronal structure. On a short timescale (from a few hours to 1 day), such reorganizations have been observed following filament eruptions or *disparitions brusques* (Watanabe et al. 1992; McAllister et al. 1992; Tsuneta et al. 1992; Watanabe et al. 1994; Khan et al. 1994; Hanaoka et al. 1994). In some cases small, transient coronal hole formations were reported related to such events (Watanabe et al. 1992, 1994). Coronal depletion related to an expanding loop structure and coronal mass ejections seen above the limb were reported by Tsuneta (1996) and Hudson et al. (1996). Such depletions might be seen as coronal hole formations when observed on the disk.

In this Letter, we present a disk event. Through X-ray, multifrequency metric radio, and magnetic observations, we show a reorganization of the coronal structure, including the formation of two coronal holes caused by an expanding twisted

flare loop. Coinciding with the spectacularly twisted expanding loops, sporadic radio type III bursts were observed spreading over an area of almost one-third the solar disk. A pair of X-ray brightenings appeared  $\sim 6'$  distant from the active region during the time of the radio bursts, and new X-ray loop connections formed between the active region and the places of those remote quiet-Sun brightenings at the borders of the new coronal holes. The timing and location of events, combined with the overall magnetic configuration, provide evidence for a large-scale magnetic reconnection occurring between the expanding twisted loops and overlying transequatorial loops that interconnect quiet solar regions.

### 2. OBSERVATIONS

The Nançay Radioheliograph (NRH; see Radioheliograph 1989), operating in the frequency band 160–450 MHz, provided the location and intensity of the burst at five altitudes between  $0.3$  and  $1 R_\odot$  above the photosphere (Radioheliograph 1989; Suzuki & Dulk 1985) whereas the soft X-ray features (Švestka 1981), outlining magnetic loops of  $1.5$ – $8$  MK temperature and density greater than  $10^8 \text{ cm}^{-3}$ , occur closer to the photosphere in the corona, at a height  $\leq 0.2 R_\odot$ . The *Yohkoh* Soft X-ray Telescope (SXT; see Tsuneta et al. 1991) measurements reported here show a system of strongly twisted, expanding magnetic loops from the onset of the long-duration C4.7 flare,  $\sim 0949$  UT on 1994 October 25, at the location S06 W11. Figure 1 shows the *GOES* soft X-ray light curve, and Figure 2 (Plate L13) displays X-ray images of the Sun just before, during, and at the end of the flare. Two

<sup>1</sup> Observatoire de Paris, Département d'Astronomie Solaire, URA CNRS 2080, Place J. Janssen, F-92195 Meudon Cedex, France.

<sup>2</sup> On leave from Radio Astronomy Centre, Tata Institute of Fundamental Research, Ooty, India.

<sup>3</sup> Konkoly Observatory, Budapest, Hungary.

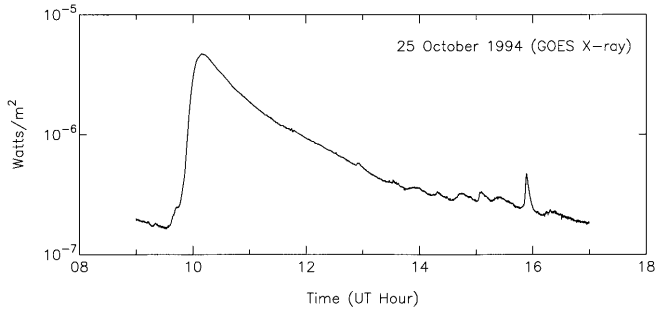


FIG. 1.—Soft X-ray GOES light curve of the flare on 1994 October 25

successive twisted expanding loops can be followed to a large angular distance from the flare's center. These loops are shown in Figures 2c and 2d. The first identified loop starts to expand (at  $\sim 300 \text{ km s}^{-1}$ ) a few minutes after the flare's onset, at  $\sim 0950 \text{ UT}$ , and the next is observed to expand ( $\sim 200 \text{ km s}^{-1}$ ) from  $\sim 0956 \text{ UT}$ . The expansion rates of these loops with respect to the flare site (active center) are plotted in Figure 3. As shown in this figure, the expansion of these loops could be followed to a distance of  $\sim 8'$  from the active center, and after that they became weaker in X-rays. Note that the observed two-sided expansion is a two-dimensional projection of a loop expanding in three dimensions.

After the beginning of the X-ray flare, the NRH measurements show a gradual increase of radio intensity above the flare site (see Fig. 4a [Pl. L14]). This continuum source continues to emit for several hours and is observed until the end of the observing period at Nançay, at  $\sim 1550 \text{ UT}$ . In addition, strong outburst activity is seen at all observing frequencies of Nançay for about 15 minutes, starting at  $\sim 1000 \text{ UT}$ . At the northeast edge of the twisted expanding loop system in the active region, radio emission of pulsating characteristics (Aurass, Klein, & Martens 1996) is observed between  $\sim 1004$  and  $1009$ . The NRH measurements also show a series of sporadic bursts in the southwest quadrant of the Sun, some of which are identified as type III bursts (caused by the high-energy electrons,  $10\text{--}100 \text{ keV}$ , accelerated and guided along open field lines starting from the corona into the solar wind at speeds of  $0.1c\text{--}0.4c$ ; Wild 1970). The positions

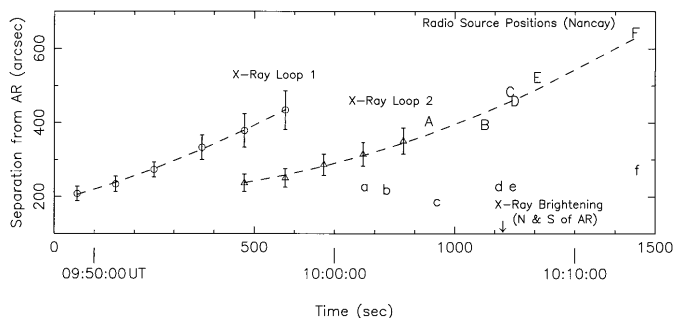


FIG. 3.—Positions of the leading edges of X-ray loops and the location of radio bursts with respect to the center of the active region as a function of time. The first (circles) and second (triangles) loops expand with speeds of  $\sim 300 \text{ km s}^{-1}$  and  $\sim 200 \text{ km s}^{-1}$ , respectively. The vertical bars indicate the typical width of the loop as it expands outward from the flare site. Locations of radio bursts are plotted for increasing time (labeled A–F). The time of the appearance of remote X-ray footpoint brightenings is also marked. Note that the bursts A–F follow the trajectory of the second expanding X-ray loop. The radio bursts marked by lowercase letters were related to events near the active region.

of these radio sources spread out from the active center, i.e., from the near-equatorial region, to larger distances (up to  $\sim 12'$ ) with time, and some are detected at high south helio-latitude,  $\sim 65^\circ$ . In Figure 4a, the locations of the radio sources measured at different observing frequencies are shown superposed on a *Yohkoh* image, and their projected angular distance from the active center as a function of time is presented together with the X-ray loop expansion in Figure 3. The positional accuracy of the NRH at these observing frequencies is better than  $0.5$ . The striking feature of the latter figure is that the successive radio locations of the bursts, marked by symbols A–F, follow the expansion of the second X-ray loop both in time and in space. Considering the projection effect, these sources are magnetically linked to a south monopolar magnetic region. For comparison, the magnetogram observed on the same day at the Kitt Peak National Observatory (see Harvey & Livingston 1970) is shown in Figure 4b. The locations of the remaining radio sources (marked by lowercase letters a–f in Fig. 3) are not reported in Figure 4. They are at an apparent distance of  $\sim 200''$  from the active center and are likely associated with the small-scale events occurring in the active region.

It is important to note that, during the radio bursts' spread-out period, two remote X-ray brightenings appear simultaneously at  $\sim 1006 \text{ UT}$  far from the flare's location (20 and 15 heliographic degrees away, toward the northwest and the southwest, respectively) and are observed until  $\sim 1020 \text{ UT}$ . These X-ray remote brightenings are indicated in Figure 2e. In the vicinity of these brightenings, two coronal holes formed (Figs. 2f and 4a), of  $\sim 15^\circ$  size in heliolongitude and helio-latitude, which were clearly visible during the following *Yohkoh* orbit (at  $\sim 1100 \text{ UT}$ ) and the next few days. Their formation is also confirmed by daily coronal maps obtained with helium spectrograph ( $1083 \text{ nm}$ ) data (Solar-Geophysical Data SESC PRT 1001). The Kitt Peak magnetogram indicates that these two new coronal hole regions are dominated by opposite polarities. These monopolar regions north and south of the flaring active center extend  $\sim 30^\circ$  in longitude, toward the northeast and southeast, respectively, from the regions where the coronal holes were formed. It is likely that, prior to the formation of these coronal holes, these opposite magnetic polarity regions were magnetically connected by an arcade of large-scale loops. These preflare loops are not seen in the *Yohkoh* SXT images, probably because they are usual coronal loops with insufficient temperature, density, or both to make them visible in soft X-rays. The darkness of the new coronal holes increased slowly with time, indicating that after the opening of the field lines, it takes some time ( $\sim 30$  minutes) to evacuate the region and reach lower density.

### 3. INTERPRETATION AND CONCLUSIONS

The above observational results show that the successive locations of the radio sources follow the expansion of the X-ray loop. Further, the simultaneous X-ray remote brightenings following the expansion and formation of two coronal holes at the brightening locations indicate the occurrence of magnetic reconnections at two levels in the corona: the first occurs in the active region, and the second reconnection process involves an interaction between the active region and the surrounding magnetic fields. The first reconnection can be understood in a three-dimensional model (Démoulin, Priest, & Lonie 1996), which implies the formation of two sets of

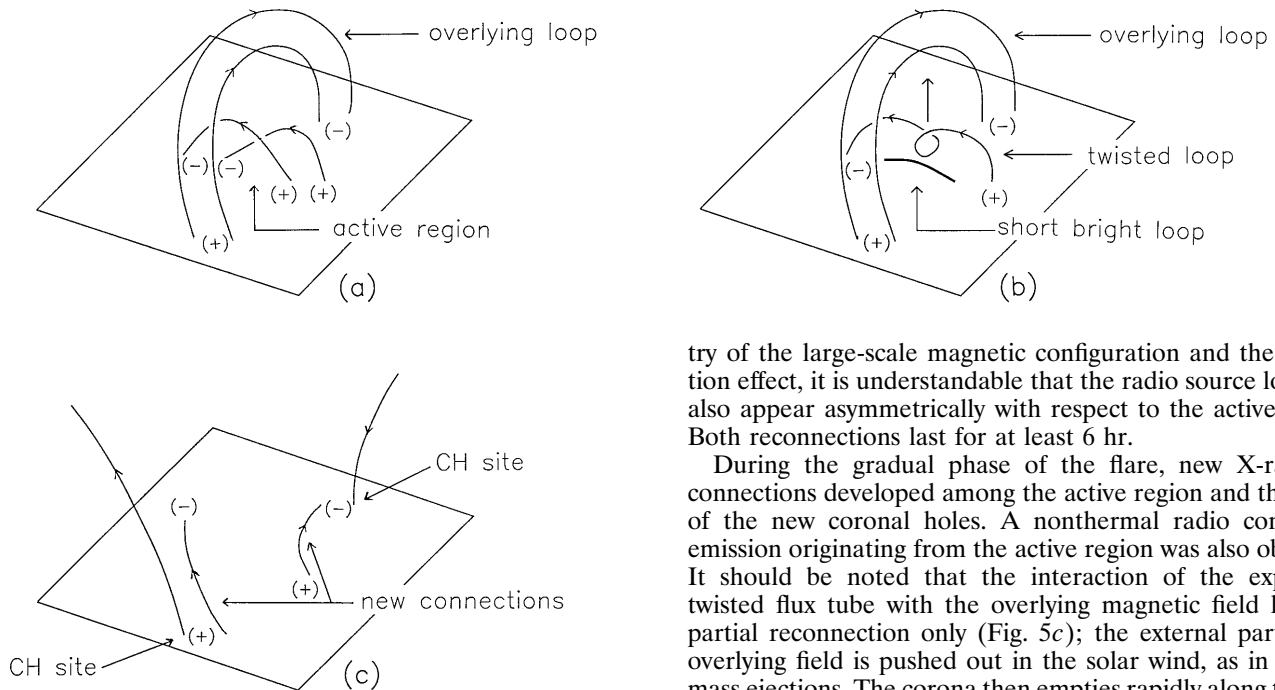


FIG. 5.—Illustrations of the magnetic field configurations discussed in § 3. (a) Magnetic field configuration before the first reconnection at the active region. The overlying loops are transequatorial loops connecting opposite-polarity quiet-Sun regions north (negative) and south (positive) (cf. Fig. 4). (b) After the first reconnection and before the second reconnection. The first reconnection causes the formation of a twisted loop and a short, brighter loop as shown. The twisted flare loop becomes unstable and starts expanding. It should be noted that radio sources are located above the photosphere at altitudes less than  $1 R_{\odot}$ , which essentially depends on the local coronal density conditions and magnetic field configuration. (c) Configuration after large-scale reconnection. New connections are created between the active region and the monopolar regions. The reconnection was only partial; the external part of the overlying large-scale fields were pushed out in the solar wind by the expanding twisted loops, leading to opening of field lines and consequent formation of the coronal holes.

reconnected hot loops: a set of short, brighter loops underneath large fainter, twisted loops. Figure 5 shows illustrations of the proposed scenario. In Figure 2, the observed twisted loop and short loops are indicated on the *Yohkoh* image. The twisted loops become unstable and start to expand. The observations of these two sets of loops in X-rays and the overlying nonthermal radio continuum radiation (brightness temperature of several hundred megakelvins) provide evidence for the first reconnection (Figs. 2 and 4). The second reconnection starts when the expanding loops reach the altitude of overlying large-scale arcade  $\sim 15$  minutes after the flare's onset (Fig. 5b). The following observational findings provide evidence for the second reconnection process: (1) remote X-ray brightenings observed in north and south monopolar regions (Figs. 2e and 4), which are assumed to represent the footpoints of large reconnected loops, (2) formation of large-scale connections (seen in the later X-ray images) between the active region and the remote quiet regions (Fig. 2f), which could only be created by magnetic reconnection, and (3) the radio-emitting sources detected toward the south of the active center above the monopolar region are found to be related, in both space and time, to the expanding X-ray flare loops (Fig. 3). Because of the asymme-

try of the large-scale magnetic configuration and the projection effect, it is understandable that the radio source locations also appear asymmetrically with respect to the active center. Both reconnections last for at least 6 hr.

During the gradual phase of the flare, new X-ray loop connections developed among the active region and the edges of the new coronal holes. A nonthermal radio continuum emission originating from the active region was also observed. It should be noted that the interaction of the expanding twisted flux tube with the overlying magnetic field leads to partial reconnection only (Fig. 5c); the external part of the overlying field is pushed out in the solar wind, as in coronal mass ejections. The corona then empties rapidly along the field lines, which is consistent with the formation of new coronal holes at large distances from the flare site. These coronal holes are indicated on the *Yohkoh* image (Fig. 2f). This is the first clear evidence of the formation of coronal holes following the ejection of twisted loops. Earlier, only a few cases of coronal depletion have been reported in association with an expanding loop and coronal mass ejections (Tsuneta 1996; Hudson et al. 1996). The acceleration of particles, observed above the flare site as enhanced radio continuum emission during several hours following the flare's onset, indicates that the sheared magnetic configuration goes through various stages of instability interacting with the surrounding field and continues to partially open the coronal magnetic field.

The above scenario is in agreement with the detection of energetic electrons (42–65 keV) associated with this flare by

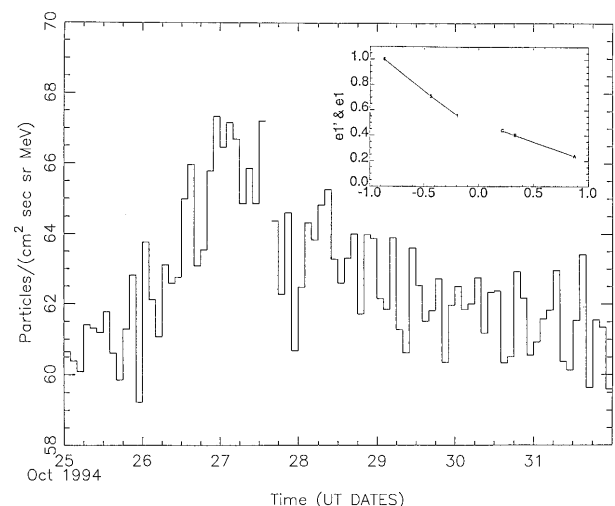


FIG. 6.—Two hour average electron fluxes of the *Ulysses* HISCALE measurements (42–65 keV) for 1994 October 25–31, using the data presented in Fig. 1 of Pick et al. (1995). Inset: Normalized (to the maximum flux) angular distribution, plotted as a function of the cosine of the pitch angle.

*Ulysses* at 2 AU distance, having its footpoint at 74° south heliolatitude and 20° east heliolongitude (Pick et al. 1995). Figure 6, using data from Figure 1 of Pick et al. (1995), shows the electron flux for the dates 1994 October 25–31. These authors estimated that the onset time of the particle event was between 1200 and 1900 UT on 1994 October 25 and the electron flux maximized nearly 1 day later than that of the flare. However, the Unified Radio and Plasma Wave (URAP) experiment aboard *Ulysses* recorded the radio emission at several distances from the Sun in the interplanetary medium caused by the fast-moving flare electrons starting from the onset time of the flare (see Fig. 2a of Pick et al. 1995). The increase of electron flux for ~1 day may be due to the fact that the reconnection continued at the active center for a long time. Thus the results presented in this Letter show that flares can trigger large-scale reconnection and reconfiguration of the coronal structure, with direct implications for the interplanetary medium.

We acknowledge H. S. Hudson and W. van Driel for helpful comments, and we thank the HISCALE *Ulysses* team for helpful discussions. P. K. M. wishes to thank the Centre Franco Indien pour la Recherche Avancée (CEFIPRA) for financial support to visit the Observatoire de Paris, Meudon. L. v. D.-G. was partially supported by Hungarian research grant T17325 OTKA I/7. The Unité Scientifique de Nançay (Nançay Radio Observatory) of the Observatoire de Paris is associated with the French Centre National de Recherche Scientifique (CNRS) USR B7040 and acknowledges the financial support of the Région Centre. We acknowledge the Centre National d'Etudes Spatiales (CNES) for its financial support. We thank the *Yohkoh* team and Mullard Space Science Laboratory for providing the X-ray data. The NSO/Kitt Peak magnetogram data used in the Letter were produced cooperatively by NSF/NOAO, NASA, GSFC, and NOAA/SEL, courtesy of Karen L. Harvey. We also thank the referee for critical comments and useful suggestions.

#### REFERENCES

- Aurass, H., Klein, K.-L., & Martens, P. C. H. 1996, in Proc. *Yohkoh* Conf. on Observations of Magnetic Reconnection in the Solar Atmosphere, in press
- Démoulin, P., Priest, E. R., & Lonić, D. P. 1996, *J. Geophys. Res.*, 101, 7631
- Hanaoka, Y., et al. 1994, *PASJ*, 46, 205
- Harvey, J., & Livingston, W. 1970, *Sol. Phys.*, 10, 283
- Hudson, H. S., et al. 1996, in IAU Colloq. 153, *Magnetodynamic Phenomena in the Solar Atmosphere*, in press
- Khan, J. I., et al. 1994, in *X-Ray Solar Physics from Yohkoh*, ed. Y. Uchida, T. Watanabe, K. Shibata, & H. S. Hudson (Tokyo: Universal Acad.), 201
- McAllister, A., et al. 1992, *PASJ*, 44, L205
- Pick, M., et al. 1995, *Geophys. Res. Lett.*, 22, 3377
- The Radioheliogroup. 1989, *Sol. Phys.*, 120, 193
- Strong, K. T. 1994, in Proc. Kofu Symp., ed. S. Enome & T. Hirayama (Nobeyama Radio Obs. Rep. 360), 53
- Strong, K. T., et al. 1994, *Space Sci. Rev.*, 70, 133
- Švestka, Z. 1981, in *Solar Flare Magnetohydrodynamics*, ed. E. R. Priest (London: Gordon & Breach), 47
- Suzuki, S., & Dulk, G. A. 1985, in *Solar Radiophysics*, ed. D. J. McLean & N. R. Labrum (Cambridge: Cambridge Univ. Press), 289
- Tsuneta, S. 1996, *ApJ*, 456, 840
- Tsuneta, S., et al. 1991, *Sol. Phys.*, 136, 37
- , 1992, *PASJ*, 44, L211
- Watanabe, T., et al. 1994, in *X-Ray Solar Physics from Yohkoh*, ed. Y. Uchida, T. Watanabe, K. Shibata, H. S. Hudson (Tokyo: Universal Acad.), 207
- , 1992, *PASJ*, 44, L199
- Wild, J. P. 1970, *Proc. Astron. Soc. Australia*, 1, 365

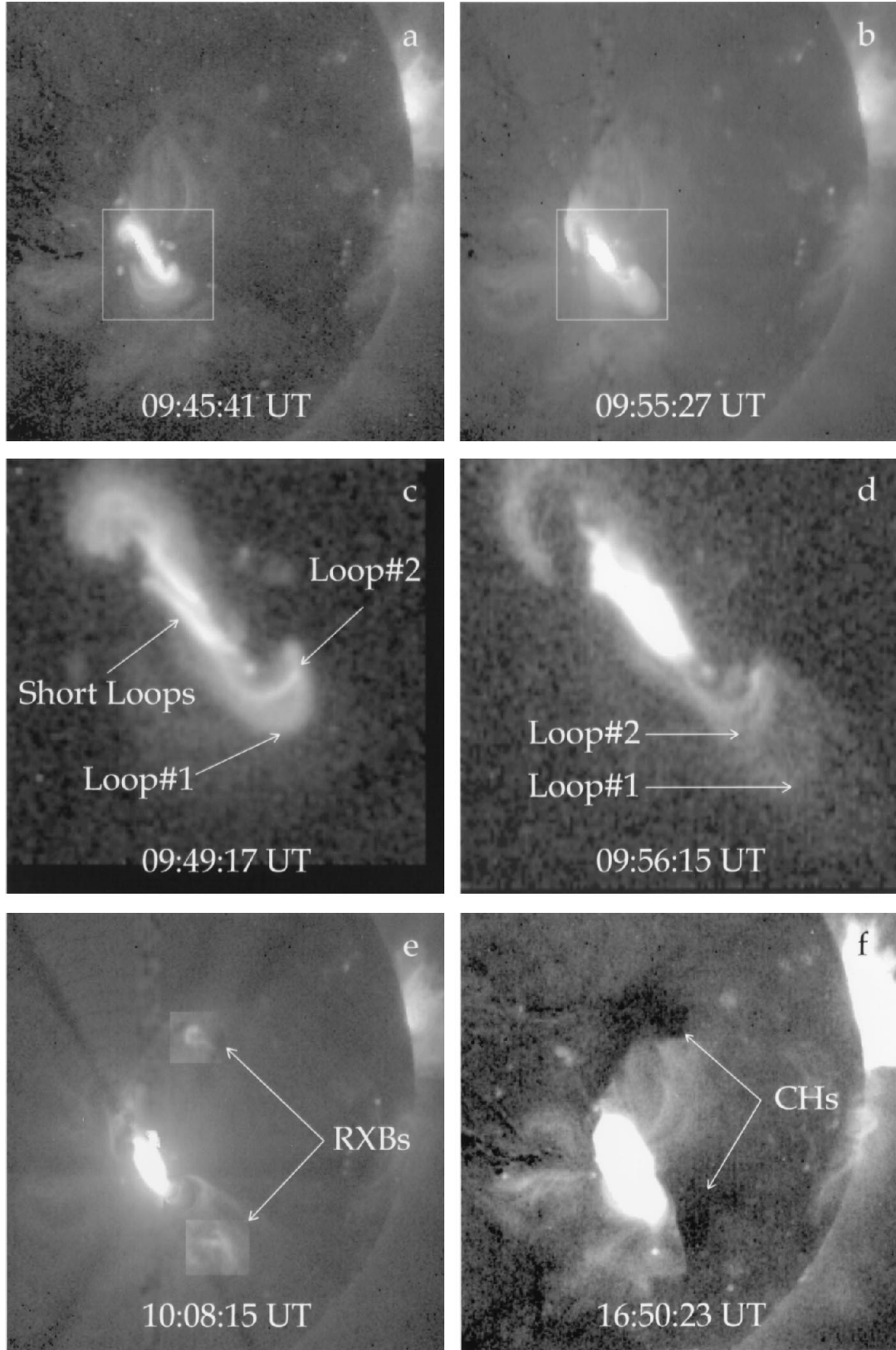


FIG. 2.—Soft X-ray images of the Sun on 1994 October 25 at six different epochs starting at 0945 UT. (a) Before the flare's onset; twisted magnetic loop structure is seen at the flare site, nearly  $11^\circ$  east and  $6^\circ$  south from the center of the Sun. (b) The twisted loop expands. (c, d) Partial frame (full resolution,  $2''45 \text{ pixel}^{-1}$ ) images of the active region, showing the observed features. Note that the field of view of these images is indicated by a box in (a) and (b). (e) Two remote X-ray brightenings are seen northwest and southwest of the active center. Note that the full picture is a composite image of two consecutive images of different exposure time, while the brightenings were inserted from the long-exposure image. (f) Near these two positions, two coronal holes are formed. New loops are also seen connecting the active center and the remote quiet regions.

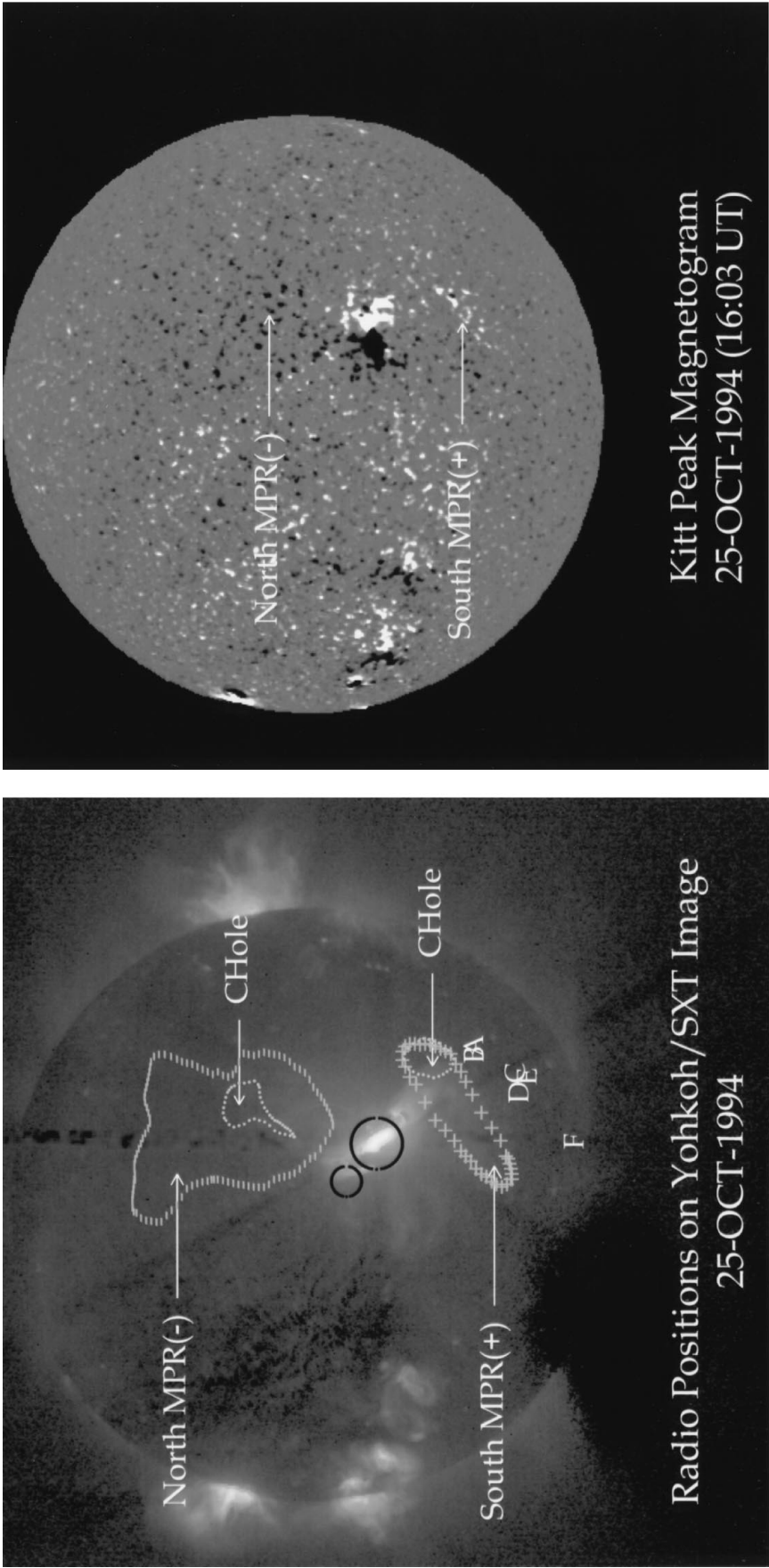


FIG. 4a

FIG. 4b

FIG. 4.—(a) Projected positions of the radio bursts superposed on the Yohkoh image observed at  $\sim 0957$  UT on 1994 October 25. The symbols A–F indicate an increasing time sequence (see Fig. 2). Regions of continuum emission and pulsating radio bursts northeast of the active center are shown as a large and a small circle, respectively. The monopolar positive and negative magnetic field regions (from the KPNO magnetogram) are outlined by the corresponding symbols (north, *minus signs*; south, *plus signs*). New coronal holes formed after the flare are indicated by dotted lines (“CHole”). Taking projection effects into account, the bursts A–F appear above the positive monopolar magnetic region. (b) Magnetogram observed on the same day at KPNO.

MANOHARAN et al. (see 468, L74)